BIOCHEMISTRY
including biophysical chemistry & molecular biology

Article

pubs.acs.org/biochemistry

TNFR1 Signaling Is Associated with Backbone Conformational Changes of Receptor Dimers Consistent with Overactivation in the R92Q TRAPS Mutant

Andrew K. Lewis, Christopher C. Valley, and Jonathan N. Sachs*

Department of Biomedical Engineering, University of Minnesota, Twin Cities, Minneapolis, Minnesota 55455, United States

Supporting Information

ABSTRACT: The widely accepted model for tumor necrosis factor 1 (TNFR1) signaling is that ligand binding causes receptor trimerization, which triggers a reorganization of cytosolic domains and thus initiates intracellular signaling. This model of stoichiometrically driven receptor activation does not account for the occurrence of ligand independent signaling in overexpressed systems, nor does it explain the constitutive activity of the R92Q mutant associated with TRAPS. More recently, ligand binding has been shown to result in the formation of high molecular weight, oligomeric networks. Although the dimer, shown to be the preligand structure, is thought to remain present within ligand−receptor networks, it is unknown whether network formation or ligand-induced structural change to the dimer itself is the trigger for TNFR1 signaling. In the present study, we investigate the available crystal structures of TNFR1 to explore backbone dynamics and infer conformational transitions associated with ligand binding. Using normal-mode analysis, we characterize the dynamic coupling between the TNFR1 ligand binding and membrane proximal domains and suggest a mechanism for ligand-induced activation. Furthermore, our data are supported experimentally by FRET showing that the constitutively active R92Q mutant adopts an altered conformation compared to wild-type. Collectively, our results suggest that the signaling competent architecture is the receptor dimer and that ligand binding modifies domain mobilities intrinsic to the receptor structure, allowing it to sample a separate, active conformation mediated by network formation.

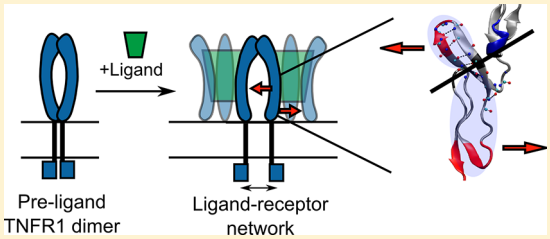

Tumor necrosis factor (TNF) receptor 1 (TNFR1) is the prototypical member of the TNFR superfamily, a family of roughly 20 type I transmembrane receptors[1] whose functions include triggering apoptosis,[2] inflammation response,[3] and cell survival.[4] TNFR1 is activated by binding one of two cognate ligands, TNFα or lymphotoxin-α (LTα, also called TNFβ), via its extracellular domain.[5] Upon ligand binding, a yet uncharacterized rearrangement of TNFR1 in the extracellular domain results in signal transduction across the membrane, causing the TNFR1 intracellular death domain to shed the silencer of death domain (SODD)[6] and subsequently bind to TNF receptor associated death domain (TRADD).[7] The signaling cascade culminates with NF-κB activation and inflammation response.[8] A less common outcome occurs in certain cell types and culture conditions wherein TRADD recruits Fas associated death domain (FADD), resulting in caspase activation and apoptotic cell death.[9] However, TNFR1 is most commonly associated with its inflammation pathway.

Abnormal TNFR1 activity is linked to a number of diseases including rheumatoid arthritis,[10] TNF receptor associated periodic syndrome (TRAPS),[11] Crohn's disease,[12] carotid thickening, myocardial infarction,[13] deep vein thrombosis,[14] and diseases of the central nervous system including multiple sclerosis.[15] These diseases have been linked to a number of polymorphisms in the extracellular domain which cause abnormal folding, oligomerization, trafficking, and shedding behavior. Additionally, most mutants are unable to bind ligand. Notable exceptions are the R92Q and P46L mutations, which are termed "nonstructural polymorphisms" in that they bind ligand, traffic, and shed like wild-type, but exhibit abnormal, ligand-independent activity and lead to disease symptoms, albeit milder ones.[16] Common treatments for TNFR1 associated inflammatory diseases include etanercept, adalimumab, and infliximab.[17] Each of these drugs reduces symptoms by competitive inhibition, capturing free ligand and rendering it unable to bind receptor. However, no current treatments act directly on the TNF receptor, which may reflect a lack of knowledge regarding extracellular signaling mechanisms involving TNFR1. Therefore, a detailed understanding of the mechanism by which ligand binding to TNFR1 results in signal transduction across the membrane may provide valuable insight into targeting TNFR1.

While downstream events of the TNFR1 signaling pathway are well characterized, the mechanism by which ligand induces signaling across the membrane—i.e., ligand-independent receptor activation and ligand-induced reorganization in the membrane—is poorly understood. Therefore, the fundamental relationship between the structure and function of TNFR1 is of

Received: May 21, 2012
Revised: July 13, 2012
Published: July 16, 2012

dx.doi.org/10.1021/bi3006626 | *Biochemistry* 2012, 51, 6545−6555

great interest. TNFR1 is comprised of an N-terminal extracellular domain, a single-pass α-helical transmembrane (TM) domain, and a cytosolic death domain. Within the extracellular domain, two distinct regions of the receptor serve two main functions, preligand assembly of monomeric receptor units[18] and ligand-binding of these preassembled complexes.[19] Ligand-independent assembly (Figure 1A) is driven through

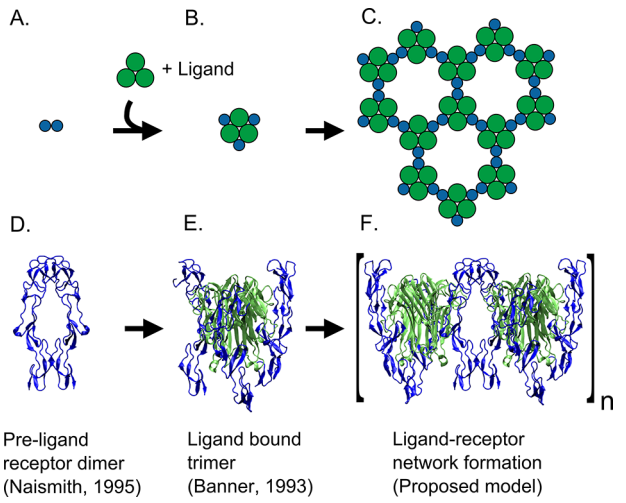

Figure 1. Ligand–receptor network model. The components of the TNFR1 hexagonal network are shown schematically with accompanying crystal structures. The receptor exists on the cell surface as a preligand dimer (A,D). The trimeric ligand binds to three receptor protomers with trifold symmetry (B,E). However, this structure is not found in cross-linking studies, rather the ligand causes the formation of high molecular weight oligomers, modeled as a hexagonal lattice (C). The dimer of trimers subunit (i.e., a pair of ligand-bound trimers associated via the receptor dimerization interface) is the smallest networked unit (F).

the membrane-distal preligand assembly domain (PLAD), and deletion of these residues has been shown to prevent the homomeric association of TNFR1 monomers.[18] Ligand binding (Figure 1B) is driven through two receptor loops which provide high-affinity, high-specificity binding via a number of noncovalent interactions.[20] Recent evidence has suggested that in TNFR1, as well as other closely related proteins including TNF-related apoptosis-inducing ligand receptor 2 (TRAIL2, death receptor 5, DR5),[21] ligand-independent interactions and ligand binding occur together to generate highly organized network structures (Figure 1C),[22] discussed further below. However, it is still unknown how the transition from a ligand-independent structure to a ligand-bound structure leads to signal transduction across the membrane.

TNFR1 is the only member of the TNFR superfamily for which crystal structures exist for both its ligand unbound (Figure 1D) and ligand bound (Figure 1E) states, albeit the extracellular domain only. The first structure solved was that of the TNFR1 ectodomain in complex with its ligand, LTα (PDB ID 1tnr, Figure 1E), revealing that the homotrimeric ligand binds symmetrically to three noninteracting TNFR1 protomers, with each protomer fitting into the groove between adjacent ligand chains.[20] This trimeric, axisymmetric LTα–TNFR1 complex agrees with previous experimental evidence for 3:3 ligand–receptor binding stoichiometry and is often considered to be the signaling complex.[23] The receptor itself is comprised of a chain of four cysteine-rich domains (CRDs), with each CRD stabilized by three pairs of disulfide-linked cysteine residues.[24] The ligand contacts are confined to CRD2 and CRD3. More specifically, ligand–receptor interactions in the receptor protomer are dominated by a loop at residues 77–81 and the turn of a β-hairpin between residues 107–113.[20]

A second crystal structure was later solved for the TNFR1 ectodomain preligand homodimer (PDB ID 1ncf, Figure 1D).[25] An antiparallel dimer structure was also solved, but is not generally believed to be relevant in a native biological system. The dimer structure reveals that in the absence of ligand TNFR1 self-interacts with extensive dimer interactions in CRD1, the PLAD. In fact, only a single dimer interaction is found outside of the PLAD, a pair of hydrogen bonds between opposite Glutamines at residue 133. The significance of this pair of hydrogen bonds is unknown.

Despite there being crystal structures solved for TNFR1 in both its ligand-independent and ligand-bound forms, the relevant signaling mechanism at the level of receptor activation—that is, the transition from a ligand-independent dimer to a ligand-bound trimer—is still not known. Comparison of the two crystal structures, 1ncf and 1tnr, has not previously revealed any definitive tertiary structural difference between the ligand-independent and ligand-bound receptor.[25] Moreover, it is notable that the ligand binding domain and the PLAD are on opposite faces of the receptor, and a structural alignment of the two crystal structures reveals that the homodimer can survive ligand binding without masking the dimerization interface or producing steric interference (Figure 1F). Despite these domains being structurally distinct, their functions have largely been considered intrinsically linked. Deletion of the membrane-distal PLAD prevents ligand binding and function, and therefore it is presumed that ligand-independent receptor assembly is a prerequisite for ligand binding and function.[26] However, these studies are largely based upon receptor mutational analysis whereby entire protein domains are removed, which could influence the structure of ligand-binding regions. The structures of sequential CRDs are interdependent and folding of TNFR1 is highly sensitive to mutation.[16] Therefore, the relationship, if one exists, between the preligand assembly domain and the ligand binding domain is yet unclear.

Nevertheless, ligand binding and dimerization do not appear to be mutually exclusive. Consequently, ligand binding does not necessarily result in the formation of a trimer, but an extended network of ligand/receptor complexes. Indeed, a cross-linking study by Chan et al. shows that ligand binding results in the appearance of high molecular weight oligomers, rather than the expected trimer/trimer complex.[18] Our recent work has emphasized specific ligand-induced receptor dimerization within the network structure of TRAIL in complex with DR5, a structurally homologous TNF ligand–receptor pair.[21] However, despite well-defined crystallographic structural data for the TNFR1 homodimer, its role within the TNFR1-LTα network has not yet been characterized. The model proposed by our group and others is a hexagonal lattice wherein the ligand bound trimer forms each vertex and the receptor homodimer forms each edge (Figure 1A–C).[21,22,27,28]

Because of the structural similarity between receptor protomers in 1ncf and 1tnr, an all-atom representation of such a network can be generated by structural alignment of the crystal structures (Figure 1F). The trifold symmetry of the ligand/receptor complex leads to a hexagonal geometry as modeled. However, a conflict becomes apparent upon

generation of the network through receptor−receptor dimerization of ligand−receptor trimers (i.e., "dimer of crystal structure trimers") shown in Figure 1F. An overlay of the crystal structures producing the dimer of trimers structure reveals a tilt of ∼35° between adjacent trimers so as to prevent this network from forming on a membrane that is essentially planar on the scale of protein geometry. Therefore, we propose a ligand-induced conformational change that causes the network to become planar and permit its formation as observed in experimental studies. We use normal-mode analysis, a powerful computational tool that has been used to accurately describe structural transitions in a variety of proteins,[29−31] to explore the conformational dynamics involved in ligand binding of TNFR1. Our observations are supported in part by our experiments and should inspire additional experiments in the future. In the present study, we investigate the backbone conformational dynamics of TNFR1, how they relate to signaling, and potential connections to ligand−receptor network formation.

METHODS

Comparison of Crystal Structures. All protein coordinates were obtained from the Protein Data Bank (PDB ID 1ncf and 1tnr). The structural alignments and root-mean-square deviations (RMSD) were calculated using the RMSD Calculator extension of VMD.[32] The calculations were performed on the backbone atoms of the indicated residues of both 1ncf chains (chains A and B) and the 1tnr receptor chain (chain R).

Normal Mode and RMSF Calculation. We calculated the full set of 3N normal modes for the Cα representations of the 1ncf and 1tnr crystal structures using the anisotropic network model tool, applying an exponential spring function, in LOOS.[33] The 1ncf chains were truncated to contain residues 14−150 for the purpose of symmetry, and the trifold symmetric 1tnr structure was kindly provided by David Banner.

The output eigenvectors and eigenvalues were used to calculate the mean-square residue fluctuations according to

$$\Delta r_i^2 \propto \sum_v \frac{e_i^2(v)}{\omega_v^2} \tag{1}$$

where $e_i(v)$ and ω_v are the eigenvectors and angular frequency, respectively, of the dynamical matrix corresponding to atom i and mode v.

Cross-Correlation Calculation. Cross-correlation maps were calculated over the first 100 nonzero frequency normal modes according to

$$C_{i,j} = \frac{\sum_1^k \frac{e_i \cdot e_j}{\omega_k^2}}{\left(\sum_1^k \frac{e_i \cdot e_i}{\omega_k^2}\right)^{1/2}\left(\sum_1^k \frac{e_j \cdot e_j}{\omega_k^2}\right)^{1/2}} \tag{2}$$

where e_i and e_j correspond to the eigenvectors of residues i and j, respectively, and ω_k is the angular frequency of the kth normal mode. Convergence was estimated by taking the Euclidean norm of the cross-correlation matrix.

FRET. pEYFP-N1 and pECFP-N1 vectors were a kind gift from David Thomas. The fluorophores had been previously mutated (A206K) to prevent dimer formation.[34] cDNA encoding TNFR1 was inserted at the n-terminus of the pEYFP-n1 and pECFP-n1 vectors using standard cloning technique. The TNFR1 sequence was truncated immediately downstream of the transmembrane domain such that the cytosolic domain was replaced with EYFP or ECFP. The R92Q mutation was introduced using standard point-mutagenesis technique and sequenced for verification.

HEK 293 cells were plated at 1:12 in a 6-well plate and transfected 48 h later as follows. 0.5 μg of ECFP-TNFR1 and 1.5 μg of EYFP-TNFR1 were diluted into 25 μL of 20 mM HEPES. A second solution of 50 μg/mL polyethylenimine (branched, MW ∼ 25 000) in 20 mM HEPES was prepared. The two solutions were mixed at 1:1 by pipetting repeatedly and incubated at room temperature for 30 min. Cells were gently washed twice and resuspended in serum-free DMEM. The DNA solution was added (50 μL total volume into each well of a 6-well plate), and the cells were incubated 4 h at 37 °C. The cells were then washed twice and incubated in serum-containing DMEM for 20 h. Immediately prior to FRET imaging, cells were lifted by gentle trypsinization and replated on poly(D-lysine)-coated plates.

Live-cell FRET imaging was conducting using a Nikon Eclipse TE200 inverted microscope and a 40× objective fitted with a mercury lamp (XCite 120 W Fluorescence Illumination Sytem). Filters for excitation and emission of CFP (430/24 and 470/24 nm, respectively) and YFP (500/20 and 535/30 nm, respectively) were controlled using an automated filter wheel (Ludl MAC6000). Images were acquired using MetaMorph and analyzed with ImageJ. Energy transfer was measured by acceptor-selective photobleaching. Briefly, cells were imaged in the EYFP and ECFP channels every 20 s for 3 min. Between image captures, acceptor was bleached by continuous exposure through the EYFP excitation channel. FRET efficiency was calculated as the intercept of the linear fit of normalized EYFP fluorescence plotted against normalized ECFP enhancement with typical R^2 values of around 0.90. The FRET efficiencies measured from individual cells were plotted against EYFP intensity and fit to a two-parameter saturable binding curve of the form

$$E = \frac{\mathrm{FRET}_{\max}[\mathrm{EYFP}]}{K_D + [\mathrm{EYFP}]} \tag{3}$$

The model parameters were extracted to determine relative binding affinity (K_D) and maximum FRET efficiency ($\mathrm{FRET}_{\max}$) of the TNFR1 dimer.

RESULTS

Structural Differences between the 1ncf and 1tnr Receptor Crystal Structures. To determine whether specific structural differences exist between TNFR1 in its ligand-independent dimeric and ligand-bound trimeric states, we used VMD to perform a global backbone structural alignment and calculate the RMSD between the preligand 1ncf receptors and the ligand bound 1tnr receptor. We calculated the backbone RMSD on all resolved residues shared among the crystal structures (residues 15−150) between chains A and B of 1ncf and chain R of 1tnr. The preligand receptor protomers differ from each other by an RMSD of 1.12 Å, with chain B appearing slightly more curved than chain A. The RMSD between 1ncf chains A and B and 1tnr chain R are 1.68 and 1.96 Å, respectively. Naismith et al. originally reported the dimer structure and noted that the trimeric 1tnr receptor protomer solved 2 years prior by Banner et al. is slightly elongated and straighter compared to their preligand dimer structure. Nevertheless, upon global alignment of all resolved residues,

dx.doi.org/10.1021/bi3006626 | Biochemistry 2012, 51, 6545−6555

the structural differences between 1tnr and 1ncf appear to be minimal and are not consistent with our expectation of a ligand induced conformational change in the cytosolic domain (Figure 2A). However, the alignment algorithm results in structural deviations being distributed globally such that the total RMSD is minimized. If instead we assume that the dimer interface survives ligand binding and the PLAD remains rigid, it is reasonable to perform the alignment on only these residues, such that the dimer interactions remain intact. Moreover, we note that the *B*-factors of the 1ncf receptor suggest that residues 15−100 are relatively immobile compared to residues 101−150 (see Supporting Information), supporting the notion that residues involved in dimeric interactions within the PLAD are unchanged upon ligand binding if we assume preservation of the dimer. We calculated a local backbone alignment and RMSD based on only residues 15−100. While residues 15−100 align more tightly (RMSD = 0.83 Å and RMSD = 0.72 Å between chain R of 1tnr and chains A and B of 1ncf, respectively), a structural change becomes apparent in the ligand binding and membrane proximal domains (Figure 2B). The RMSDs calculated on residues 100−150 between chain R and chains A and B are similarly reduced (RMSD = 0.83 Å and RMSD = 0.79 Å respectively), again showing that the differences between the ligand bound and ligand unbound structures correspond to a rigid body motion within the receptor protomer. Specifically, we found that in 1tnr the ligand binding loop at residue 110 drops toward the membrane and that the membrane proximal domain rotates away from the dimerization interface. We then reconstructed the receptor dimer by aligning residues 15−100 of the 1tnr receptor protomer with both chains of 1ncf and found that the membrane proximal residues are substantially further apart, consistent with a conformational change in the TM and cytosolic domain (Figure 2C). These results show clearly that structural differences exist between TNFR1 in its dimeric state and ligand-bound trimeric state. Whether this structural change is truly a consequence of ligand binding or of other crystallization conditions is unknown; however, it does demonstrate a large degree of flexibility between the dimerization interface and the ligand binding and membrane proximal domains, which may be relevant to signaling in the full-length, membrane-anchored receptor.

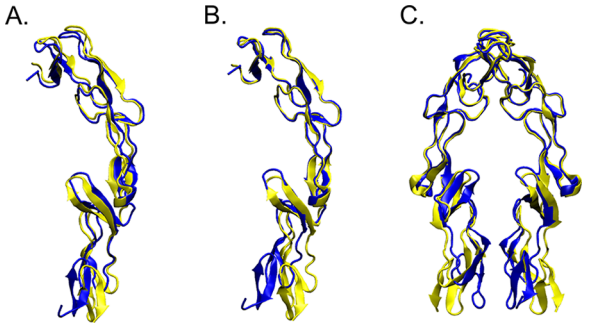

Figure 2. Alignment of the 1ncf and 1tnr receptor protomer structures. The alignment of 1ncf chain B (blue) and 1tnr chain R (yellow) shows that the global structural differences between the two structures are minimal (A). Alignment along residues 15−100 reveals a structural change in the membrane proximal residues, mediated by flexibility within the receptor chain (B). The structural change in the membrane proximal residues becomes even more apparent when the 1tnr protomer is superposed onto both chains A and B of 1ncf (C).

Comparison of the Crystal Structures Reveals Increased Flexibility in the PLAD of the Ligand-Bound Trimer. To more completely characterize the backbone mobility of the TNFR1 protomer as well as the collective motions of the tertiary structure involved in the transition from the ligand unbound dimer to the ligand bound trimer, we calculated the normal modes of both the 1ncf and 1tnr structures. To date, the dynamic behavior of the TNFR1 backbone has been largely disregarded and its relationship to signaling has not been investigated. Normal-mode analysis (NMA) is a powerful tool used to characterize the large-amplitude structural fluctuations of a protein, including conformational changes that occur on time scales not accessible by all-atom molecular dynamics. We calculated the normal modes of both structures using LOOS, which employs the anisotropic network model (ANM), reducing computational cost by coupling atoms through a single parameter energy potential in place of the traditional all-atom empirical force field.[33] ANM reveals the 3-dimensional structural properties of a protein by assuming that, while residue-specific atomic interactions guide the determination of the folded state, once folded the protein behaves to a large extent as an elastic solid, and molecular forces stabilizing the 3-dimensional geometry dominate.[35] The model is further simplified by reducing the treatment of residues to alpha-carbons only. While this appears to be an oversimplified model, normal-mode analysis has been shown to accurately predict structural changes in proteins in which multiple conformational states are known.[29,36−38]

The protomer chains of 1ncf were truncated for symmetry to include only residues 14−150. The truncated residues (11−13 and 151−155) can reasonably be omitted because they form incomplete domains with negligible intramolecular contacts and do not contribute meaningfully to the resolved portion of the tertiary structure. To analyze the relative residue fluctuation of the receptor protomer, we summed the full set of $3N - 6$ inverse-eigenvalue weighted normal modes according to eq 1. The peaks on the resulting plot show which regions of the backbone tend to be more mobile, with low-frequency collective motions dominating while high-frequency vibrations offer negligible contributions (Figure 3A). The two crystal structures show notable differences in the mobility of various protein regions.

In the all-atom representation, extensive noncovalent interactions within the PLAD of the 1ncf crystal structure at residues 47−49 stabilize the dimer interface (Figure 3A, region ii). These residues are in turn stabilized by the loop formed at residues 23−27 (region i), which does not form any dimer contacts but is structurally coupled to the dimer interface of the PLAD. Comparing the residues fluctuations from the normal-mode analysis of the homodimerized state (i.e., 1ncf) to the ligand-bound trimer state (i.e., 1tnr), both regions i and ii are more flexible in the ligand-bound state due to the loss of dimeric intermolecular interactions across the PLAD interface. While the intermolecular side chain interactions that join the dimer are not present in our coarse-grained representation, the two chains are near enough in the dimeric 1ncf structure that the exponentially decaying potential between them substantially influences the normal modes of the system. In the dimer state, these residues are surrounded by a larger number of close range interactions, and the region expectedly becomes more rigid, in agreement with the *B*-factors and justifying our treatment of the crystal structures.

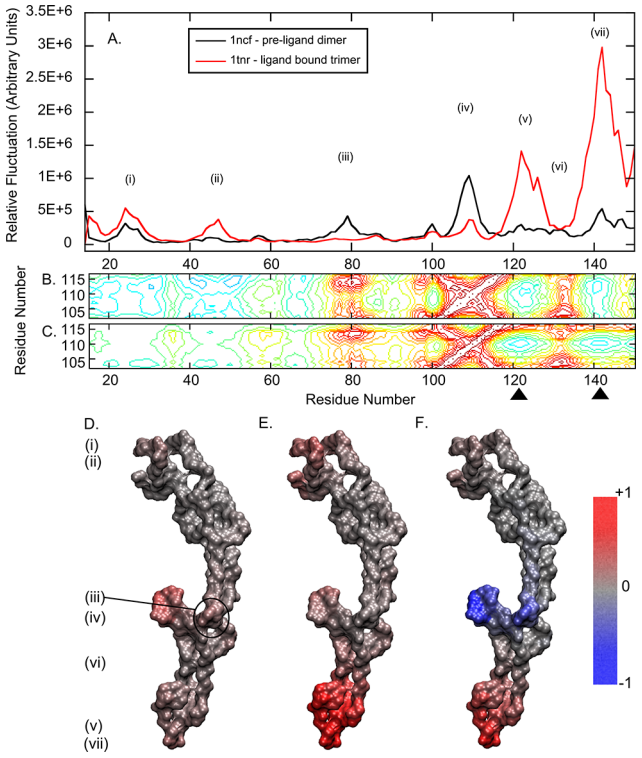

Figure 3. Normal mode analysis of the 1ncf and 1tnr structures. The residue fluctuations are shown for 1ncf (black) and 1tnr (red), summed over the full set of $3N - 6$ normal modes (A). The equal-time motional correlations are shown for residues 105−115 for 1ncf (B) and 1tnr (C). Normalized residue mobility is shown schematically for the 1ncf protomer (D) and 1tnr (E), with the difference (i.e., 1ncf mobility subtracted from 1tnr mobility) shown in (F). Relative mobility and differences in mobility are indicated according to the color bar.

The Ligand Bound State Exhibits Disparate Flexibility in the Ligand Binding Domains. The two predominant ligand binding domains of TNFR1 are formed by a loop at residues 77−81 (Figure 3A, region iii) and the turn of a β-hairpin at residues 107−113 (Figure 3A, region iv). They are coupled by a hydrogen bond between the backbone carbonyl of residue 80 and the backbone nitrogen of residue 114, which along with residue 104 transect the midpoint of the β-sheet. The midpoint of the β-sheet is further stabilized through a hydrogen bond between residues 104 and 131. Although the two ligand binding regions are tangentially coupled, they form two distinct and independent domains (Figure 4, regions iii and iv), as the essential ligand binding residues of the β-hairpin are formed distally at residues 107−108. Furthermore, the two ligand binding domains target separate sets of residues within two separate protomers of the trimeric ligand.[20]

In the dimer state, both ligand binding domains are flexible due to the absence of ligand interactions. Region iii runs along the spine of the receptor protomer and forms multiple intramolecular contacts, while the β-hairpin (region iv) projects prominently from the structure, tethered only at its midpoint. As a result, the β-hairpin is substantially more mobile. Fluctuations in residues 77−81 are fully damped when buried by ligand binding, while region iv remains somewhat flexible. If we treat the ligand as a rigid extension of the ligand binding domains, it is apparent that fluctuations in the β-hairpin would act to rotate the ligand about the rigid 77−81 loop. Conversely,

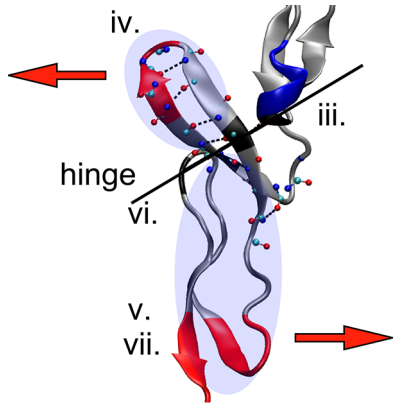

Figure 4. The ligand binding region is coupled with the membrane proximal residues. The anticorrelated ligand binding domain and membrane proximal residues are highlighted. The correlation analysis suggests that region iv and regions v and vii rotate as a rigid body about the axis defined by the immobile residues 80, 104, 117, and 133 (black line). This reveals a mechanism by which ligand-induced displacement of the ligand binding β-hairpin propagates as a structural change in the membrane proximal domains.

this shows that the ligand can reorient with respect to the principal axes of the receptor by displacing region iv while region iii remains stationary.

The Transition to the Ligand Bound State Enhances Flexibility in the Membrane Proximal Domains. Approximately 22 residues leading to the TM domain are unresolved in both solved crystal structures, and they are not believed to play a role in either ligand binding or dimerization.[25] The missing residues are expected to be highly structured, forming CRD4, which is stabilized by three pairs of disulfide-linked cysteines. The crystal structure gives coordinates for approximately half of CRD4, and we assume that the behavior of these residues reflects, or at least has direct influence on, the behavior of the rest of the domain as well as the TM helix.

The membrane proximal domains (regions v and vii) fluctuate modestly in the dimer structure, and the transition to the ligand bound state causes their mobility to increase dramatically (Figure 3A,F). That ligand binding results in such a substantial increase in the fluctuations of the membrane proximal residues is by itself evidence for ligand-induced conformational change in the TM domain; however, we sought to determine the mechanism through which ligand binding exerts this influence. A potential explanation is that dimerization contacts, though they are few and long-distance, contribute to the stability of these regions in the 1ncf structure. However, the sole dimerization interaction outside of the PLAD is a pair of hydrogen bonds formed symmetrically by apposed Q133 residues (region vi), and the mobility at this residue is unaffected by the loss of dimer. Furthermore, we later show that the membrane proximal residues are flexible even where ligand−receptor trimeric and receptor−receptor dimeric interactions are present as in the ligand−receptor network model (discussed below). Thus, the increased flexibility in regions v and vii appears to be an allosteric effect of ligand binding and not a direct result of dimer dissociation.

Motions in the 107−113 Ligand Binding Loop and the Membrane Proximal Domains Are Coupled. Comparing the fluctuations of the ligand-independent and ligand-bound crystal structures, we have shown two striking features that coincide with the transition from the ligand-independent

dx.doi.org/10.1021/bi3006626 | *Biochemistry* 2012, 51, 6545−6555

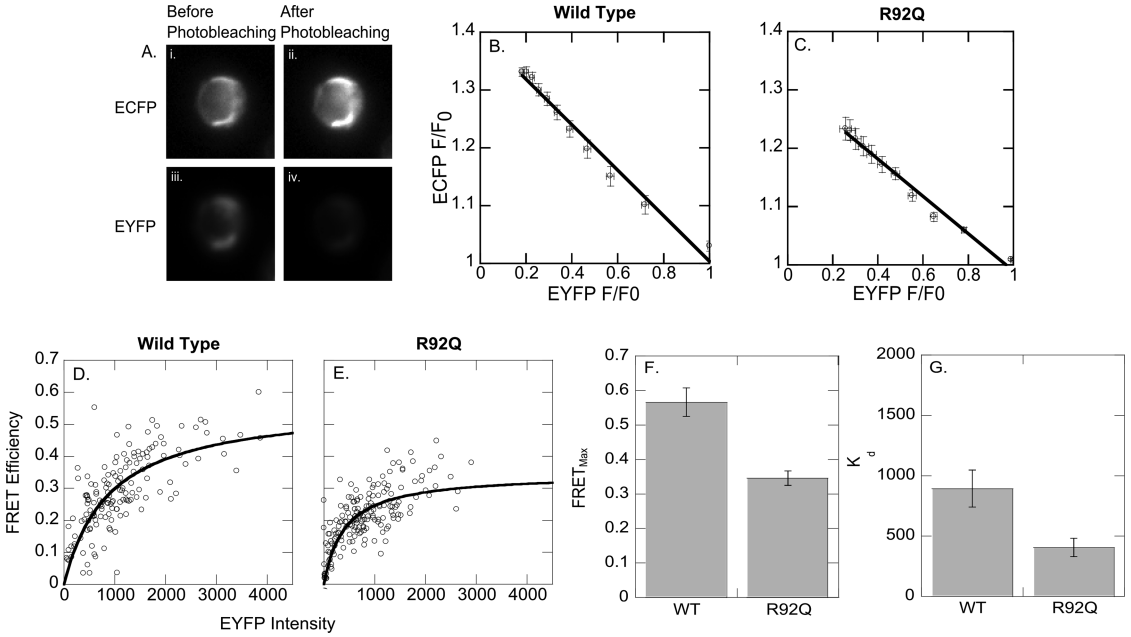

Figure 5. FRET analysis of the constitutively active R92Q mutant. Energy transfer was measured by acceptor selective photobleaching. A single cell is shown in the ECFP channel before (A, i) and after (A, ii) photobleaching, and the EYFP channel before (A, iii) and after (A, iv) photobleaching. ECFP was plotted against EYFP during the photobleach to discern the oligomeric state of the WT (B) and R92Q (C) receptors. FRET efficiencies of individual cells were plotted against EYFP intensity and fit to a two-parameter saturable binding curve for WT (D) and R92Q (E). The model parameters were extracted. $FRET_{max}$ relates to the structure of the receptor dimer (F), and K_d provides a measure of the relative affinities (G). Error bars represent the error of the fit.

receptor dimer state to the ligand-bound trimeric state. First, two regions of the TNFR1 protomer, one rigid and one flexible, bind to the ligand at two distinct sites, and second, ligand binding causes dramatically enhanced flexibility in the membrane proximal domains. In order to determine whether these phenomena are related and, if so, how the mobilities of these regions are correlated, we calculated the equal-time motional correlation between all residues pairs of the receptor protomer (for complete cross-correlation analysis of TNFR1 1ncf and 1tnr structures, see Supporting Information). The individual analysis of low-frequency normal modes provides valuable insight into large scale structural changes between functional conformations; however, the observation of correlated motions between protein domains in a single eigenvector does not necessarily imply that they are coupled over the full range of motion of the system.[39] Therefore, to understand the coupled motions of protein domains, it is necessary to calculate the cross-correlation over a sufficient range of normal modes such that the cross-correlation matrix becomes converged. We calculated the cross-correlation over the first 100 nonzero frequency normal modes according to eq 2, using the Euclidean norm as an estimate of convergence (see Supporting Information).

The cross-correlation is shown for TNFR1 residues 100–117, the mobile ligand binding β-hairpin, for both the 1ncf and 1tnr structures (Figures 3B and 3C, respectively). Qualitatively, the correlation peaks do not appear to change upon ligand binding. If we assume that the signaling competent unit is the dimer and that the ligand initiates signaling through coupled deformation of the membrane proximal region via the ligand-binding β-hairpin, this demonstrates that the ligand-independent dimer is intrinsically predisposed to the same correlated motions as the ligand-bound trimer and is thus capable of initiating signaling. What differs is the relative mobility of the ligand binding and membrane-proximal domains in each structure (Figure 3A); so while the liganded complex is flexible and may access the signaling conformation with ease, the preligand dimer is rigid and reaches the signaling conformation with relatively lower frequency. This result suggests that the ligand-independent dimer is capable of initiating signaling, consistent with results showing that unliganded TNFR1 triggers NF-κB activation when overexpressed[6] or in the case of the constitutively active R92Q mutant.[40] Moreover, ligand binding to the wild-type receptor changes the overall energy landscape, thus providing access to a range of active structures that are inaccessible (or energetically unfavorable) in the absence of ligand.

As mentioned above, residues 104 and 114 are structurally proximal and functionally related to residue 80, which is reflected by highly correlated motion between them (Figure 3B,C). Positive correlation is present between the ligand binding residues of the β-hairpin and residues 77–81; however, this appears to be an indirect effect of the strong structural coupling at the midpoint of the β-sheet. Positive correlation at residues 107 and 108 is greatly diminished compared with residues 104 and 114, suggesting that it is merely a consequence of structural proximity. Also, the mobility of residue 80 is abolished in the ligand bound state as shown in Figure 3A, so although the motions are somewhat correlated, they are negligible in magnitude and likely correspond to modest rigid body translations.

The ligand binding β-hairpin (region iv) and the membrane proximal domains (regions v and vii) are mobile (Figure 3A), and their motions are highly anticorrelated, as shown by the negative peaks localized at residues 120 and 140 (Figure 3B,C, arrowheads). That is, motion in region iv tends to cause opposite motion in regions v and vii. Recalling the structural arrangement of the immobile residues, the ligand binding

dx.doi.org/10.1021/bi3006626 | *Biochemistry* 2012, 51, 6545–6555

domain and the membrane proximal domains appear to rotate through a rigid axis defined by residues 80, 104, 117, and 133 (Figure 4). If we again consider the ligand as a rigid extension of the ligand binding domains and assume that the behavior of the TM domain is heavily influenced by that of the membrane proximal residues, it follows that reorientation of the ligand about the principal axes of the receptor may propagate through CRD4 to generate a structural change in the TM domain.

FRET. On the basis of our normal-mode analysis and comparison of the crystal structures, we predict that signaling is caused by a structural change in the receptor dimer. We experimentally tested our prediction of an active conformation by performing FRET measurements on ECFP and EYFP tagged chimeras of wild-type and mutant TNFR1. We tagged TNFR1 such that the intracellular death domain is truncated and the fluorophore is substituted in its place. Placement of the fluorophore immediately downstream of the TM domain without a flexible linker region prevents it from sampling a wide range of geometric configurations so that the distance measured between fluorophores more accurately reflects changes in the extracellular domain propagated through the membrane. While removal of the death domain abolishes the native function of TNFR1 by preventing it from binding cytosolic adapter proteins, it allows us to directly observe how the behaviors of the intracellular and extracellular domains are coupled, as we have done recently for a related family member, Death Receptor 5.[21] We measured FRET by acceptor photobleaching where the enhancement in fluorescence by the donor fluorophore after selective photobleaching of the acceptor yields a quantitative measure of the distance between the two fluorophores (Figure 5A). We take the FRET efficiency as the theoretical maximum donor enhancement at 100% acceptor bleaching (see Supporting Information).

To determine the active dimeric structure of TNFR1, we measured receptor energy transfer in a constitutively active mutant, R92Q, and compared the energy transfer to the wild-type receptor. The TNFR1 R92Q mutant is known to induce mild inflammatory symptoms in patients with TRAPS.[16] Furthermore, it has been shown *in vitro* that the R92Q mutation causes elevated basal NF-κB activation, while ligand induced NF-κB activity is comparable to wild-type.[40] We observed measurable ligand-independent energy transfer in both wild-type TNFR1 and the R92Q mutant demonstrating clearly that both wild-type and mutant receptors oligomerize within the plasma membrane. We confirmed the dimeric nature of these interactions in both the wild-type and R92Q mutant by plotting ECFP vs EYFP intensity during photobleaching (Figure 5B,C). As previously described,[41,42] dimeric donor/acceptor interactions display a linear bleaching profile between lost EYFP intensity and gained ECFP intensity, while the formation of higher order oligomers is revealed as deviation from linearity. Our ECFP vs EYFP profiles are consistent with dimeric interaction between membrane receptors, and more importantly, the degree of oligomerization is indistinguishable between wild-type TNFR1 and R92Q. Therefore, the constitutive activity observed in the R92Q mutant is the result of a receptor structural change rather than a change in receptor oligomerization.

To determine the structural difference that exists between wild-type TNFR1 and R92Q as propagated through the membrane, FRET efficiency was plotted as a function of EYFP intensity (the EYFP intensity is proportional to total receptor concentration) on a single cell basis (Figure 5D,E). The plot of FRET vs EYFP intensity shows a monotonically increasing curve, which can be fit to a two-parameter saturable binding curve as previously described.[21,34,42] From the model fit, we are able to decouple the structural properties of the receptor dimer from its dimerization affinity based on the extracted model parameters, where the $FRET_{max}$ reflects the average distance between the donor and acceptor fluorophores and the K_d provides a measure of their affinity. Interestingly, based on our model fit, R92Q dimerizes with a lower $FRET_{max}$ than the wild-type receptor, suggesting that the average fluorophore separation is greater in the mutant as compared to the wild-type receptor (Figure 5F). Moreover, R92Q dimerizes with a lower K_d than the wild-type receptor, suggesting that the mutant homodimerizes with greater affinity (Figure 5G). Though it is unknown whether the change in affinity is due to interactions involving the mutant or due to large scale changes in receptor structure, the combination of higher affinity and a change in cytosolic domain separation in the R92Q mutant may both contribute to its ligand-independent activity. Because of limitations in the maximum attainable transfection levels, there is some degree of uncertainty in the model fits due to the scarcity of data points in the plateau region at high EYFP intensity. We note that the extent to which our data populate the plateau regions in the scatter plots is similar to previously published studies using the same fitting technique.[42−44] To eliminate any bias resulting from the uneven distribution of data points, we have binned the data and refit the curves (see Supporting Information). While binning slightly diminishes the difference in both $FRET_{max}$ and K_d between wild-type and R92Q, the overall effect is unchanged. Specifically, the R92Q mutation leads to a 27% or 39% reduction in $FRET_{max}$ and a 27% or 55% reduction in K_d taken from the binned data or raw data, respectively. We also calculated the average FRET efficiency from cells expressing high levels of EYFP and found that, without depending on a model fit, the R92Q mutation leads to a significant reduction in FRET of 19%, consistent with our conclusion that the mutation causes separation of the cytosolic domains (see Supporting Information).

Collectively, our FRET results suggest that the TNFR1 R92Q mutation results in an altered structure—an open conformation with increased separation between the cytosolic domains of the receptor dimer. We propose that this open conformation adopted by R92Q is the signal competent configuration and that the same conformational change is enforced through ligand-induced binding as predicted by our normal mode and crystal structure analysis described above. However, direct measurement of ligand-induced changes in FRET is complicated by the formation of ligand/receptor networks. The formation of networks introduces multimeric donor/acceptor combinations, and it is not possible to measure the energy transfer in only the TNFR1 homodimer. While we predict a ligand-induced decrease in dimeric FRET, others have reported a ligand-induced increase in overall FRET, which may reflect the formation of such networks leading to an overall increase in energy transfer.[27] We predict that ligand binding would lead to a separation of the fluorophores in the receptor dimer that is subsumed within the network, resulting in decreased energy transfer. However, despite a reduction in dimeric energy transfer, the clustering of fluorophores due to network formation would increase overall energy transfer measured using steady-state techniques. (We estimate from the crystal structure that network formation would draw nondimer

dx.doi.org/10.1021/bi3006626 | *Biochemistry* 2012, 51, 6545−6555

receptors within 30 Å of each other, where the Förster distance of ECFP−EYFP is ∼49 Å.[45]) The net effect of these two competing contributions to FRET complicates the analysis in the presence of ligand. We do expect that ligand-induced networks would manifest as a nonlinearity in the ECFP vs EYFP bleaching profile (Figure 5B,C) due to the presence of multiple acceptors within the Förster distance of each donor molecule. Fluorescence lifetime imaging and model-based fitting algorithms are better suited for determining dimeric energy transfer in a complex system with many donor−acceptor combinations.

DISCUSSION

Because of the structural similarity between the crystal structures of the preligand, dimeric TNFR1 and ligand-bound, trimeric TNFR1, a receptor conformational change has not previously been considered as a potential trigger for signal initiation. As a result, the widely accepted model for TNFR1 activation is that ligand binding causes its trimerization, thereby resulting in a reorganization of the cytosolic domains, and that the receptor trimer is the signaling competent architecture; however, the precise molecular mechanism of TNFR1 signal initiation at the level of ligand−receptor binding is uncharacterized. Further, the current trimerization model does not account for ligand-independent signaling as in the R92Q mutant or in overexpressed systems nor does it explain the significance of ligand−receptor network formation. We have identified a potential conformational change in the receptor backbone, consistent with ligand binding and reorganization of the cytosolic domains. In this study, we provide evidence that the signaling competent architecture is the dimer and that ligand binding and network formation serve to stabilize an active dimeric conformation.

Our results are consistent with our hypothetical model in which ligand binding induces a conformational change in the cytosolic domains and forms organized networks via dimeric receptor interactions. However, the precise mechanism through which ligand displaces the ligand binding β-hairpin has not been described. Ligand binding causes TNFR1 to form networks, modeled as a hexagonal lattice as in Figure 1C. We generated a dimer of trimers model, the smallest networked subunit (Figure 1F), by structural alignment of the 1ncf and 1tnr crystal structures and found that while networks may form without steric interference between dimerization and ligand binding, the resulting structure is not planar with respect to the membrane. The principal axes of adjacent ligands in the dimer of trimers are tilted at an angle of ∼35° with respect to one another. Expansion of the network beyond two trimer subunits will result in further conflict with the membrane, forming a spiraling structure rather than the flat hexagonal structure, coplanar with the membrane as predicted (see Supporting Information). This conflict is shown schematically in Figure 6A (network tilting is shown in two dimensions for clarity). In order for the network to form, the ligand−receptor complex must undergo a structural change so that adjacent trimer subunits are coplanar with each other and with the membrane. We believe this conformational change is consistent with the observed structural difference between the inactive wild type and the constitutively active R92Q mutant in the absence of ligand and that the conformational change is consistent with the altered mobility observed in our normal-mode analysis (Figure 6B). This further suggests that the function of the receptor is dictated not by ligand-induced changes in death domain stoichiometry, as previously thought, but rather by a network stabilized conformational change in the receptor dimer.

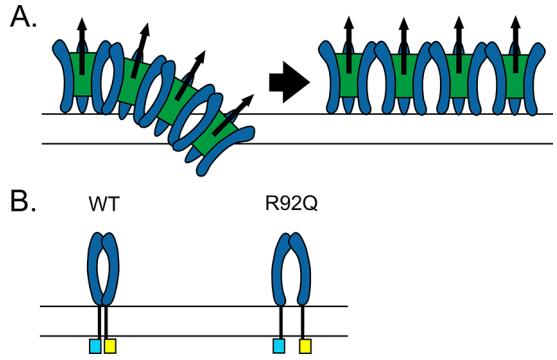

Figure 6. Receptor conformational change and network flattening. FRET analysis shows the formation of an altered conformation in the cytosolic domain in the R92Q mutant compared with wild-type. We propose that the same conformational change is induced by ligand−receptor network formation. The ligand−receptor network, as generated by structural alignment of the 1tnr and 1ncf crystal structures, results in a steric conflict with the would-be membrane. This conflict is illustrated schematically in two dimensions for clarity. Adjacent ligand trimers are tilted at an angle of ∼35°. To alleviate this steric conflict and grow the ligand−receptor network, a structural change must occur in the receptor dimer to allow the network to become coplanar with the membrane (A). The same conformational change is shown for the FRET constructs (B).

Normal mode analysis of the dimer of trimers reveals that the essential motions of network flattening can be characterized by just two low-frequency modes (Figure 7). It is important to note that the analysis of individual normal modes does not reveal the equal-time correlated motions of protein domains; however, individual modes can be useful in roughly describing large-amplitude structural changes in the protein complex. In order to flatten, the ligand trimers must rotate and separate at their membrane proximal end (Figure 7A, top) as well as swivel in the plane separating the two ligand trimer structures (Figure 7A, bottom). The top and bottom of Figure 7A show the dimer of trimers structure prior to any displacement. The flattening motions are described by normal mode 1 and normal mode 3, respectively (Figure 7B, top, and Figure 7B, bottom). Normal mode 2 corresponds to an asymmetric rotation of the dimer through an axis perpendicular to the membrane and does not contribute to flattening. After an arbitrary displacement along normal modes 1 and 3, it is apparent that the dimer of trimers becomes flat with respect to the membrane (Figure 7C, top, and Figure 7C, bottom, show the dimer of trimers structure after displacement through modes 1 and 3, respectively).

Normal mode analysis of the dimer of trimers model shows, as in 1tnr, that mobility is increased in the membrane proximal regions compared to 1ncf (Figure 8). Indeed, the membrane proximal domains at regions v and vii and the ligand binding loop at region iv become the most mobile regions of the structure (Figure 8B; red indicates mobile regions). Therefore, we propose that it is the change in the orientation of the ligand with respect to the principal axis of the receptor, enforced by network formation within the planar membrane, that displaces the mobile ligand-binding β-hairpin about the rigid ligand-binding domain at residues 77−81. We suggest that this conformational change propagates to the membrane proximal

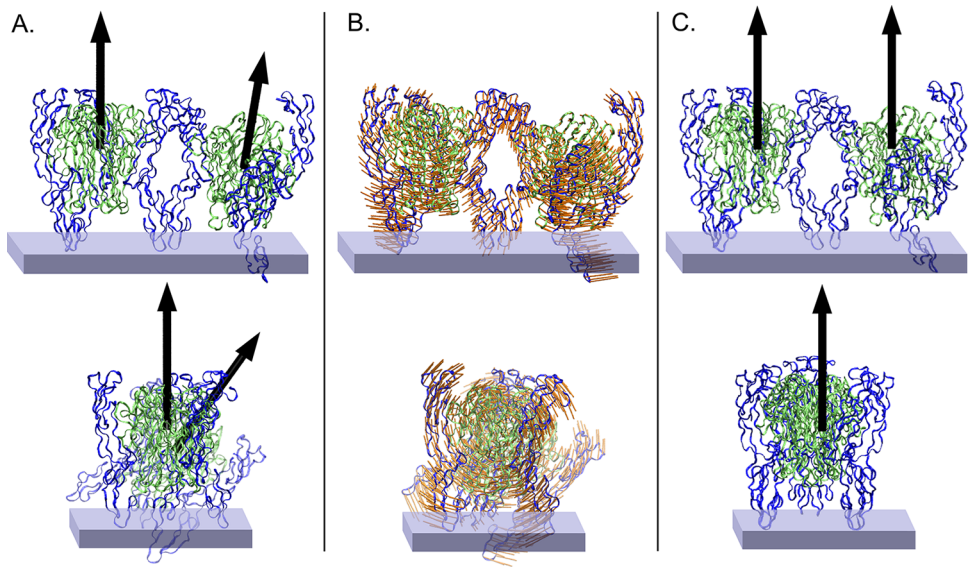

Figure 7. Normal modes of the dimer of trimers predict flattening. The dimer of trimers formed by structural alignment of the 1ncf and 1tnr crystal structures is shown from the front (A–C, top) and side-view (A–C, bottom). Both structures are shown prior to any displacement through the normal modes in panel A. Vectors are drawn corresponding to the principal axis of each ligand trimer. Porcupine plots illustrating the collective motions described by modes 1 and 3 are shown (B, top and bottom, respectively). The resulting structures after arbitrary displacement through mode 1 and 3 are flattened to permit network extension (C, top and bottom, respectively).

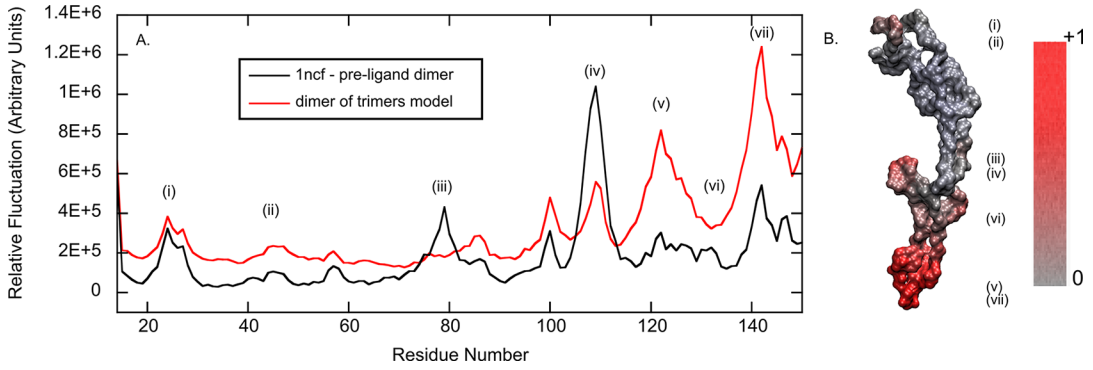

Figure 8. Relative mobility of the dimer of trimers model by residue. Relative fluctuations by residue were calculated as in Figure 3 for the dimer of trimers model. Residue mobility differs substantially compared to 1ncf (A). The relative fluctuation is shown schematically in (B).

region as illustrated in Figure 4, thereby resulting in a structural change in the TM and cytosolic domains.

We are the first to show a higher degree of separation in the cytosolic domains of a constitutively active, disease-related mutant as compared to the wild-type TNFR1. As such, we believe that separation of the cytosolic domains of the TNFR1 dimer is consistent with its activation. The mechanism coupling cytosolic domain separation with binding of adaptor proteins has not yet been explored, and no structural data exist characterizing the interaction of the TNFR1 death domain with its cytosolic adaptor proteins. However, a crystal structure has been solved revealing homodimeric organization of the TNFR1 death domain.[46] Further studies have shown that the residues involved in homotypic death domain interactions are also responsible for, or overlap with residues responsible for binding to TRADD.[47] Therefore, it is conceivable that separation of the TNFR1 cytosolic domains—that is, transition to the active state—causes dissociation of the death domain dimer and allows TRADD to bind to the previously concealed homodimerization/TRADD binding sites. The key residues involved in SODD binding have not been mapped, nor has its structure been solved; therefore, we reserve speculation on its function in TNFR1 cytosolic domain separation.

The idea of ligand induced cytosolic domain separation as a signaling mechanism has been previously investigated using FRET in integrin $\alpha_L\beta_2$.[44] Upon ligand binding to their extracellular domains, the alpha and beta subunits of the receptor dimer undergo a conformational change, resulting in "swinging out" of their cytosolic domains, and this structural change activates the receptor and initiates outside-in signaling, measured by FRET[44] and intracellular tyrosine phosphorylation.[48] A similar mechanism has been proposed for the activation of p75 neurotrophin receptor (NTR), a fellow member of the TNFR superfamily. Ligand binding is believed to result in a scissors-like movement in the receptor dimer about a disulfide hinge in the transmembrane region, causing the extracellular domains to join and the cytosolic domains to separate. This conformational change was observed using FRET, and it is believed to expose binding interfaces for downstream signaling factors.[49]

In our proposed model of TNFR1 activation, the signaling competent stoichiometric unit is the dimer. The role of the

dx.doi.org/10.1021/bi3006626 | *Biochemistry* 2012, 51, 6545–6555

ligand in mediating the separation of cytosolic domains and transition to the active state is twofold. In one respect it modifies the intrinsic structural fluctuations in the receptor backbone, allowing it to more readily sample the active conformation. This is supported by our cross-correlation map and suggests that while the TNFR1 dimer is capable of initiating signaling, it is unlikely to do so due to restricted mobility in key domains. While the ligand-independent receptor does not form networks or experience the associated flattening constraint, in certain energetically unfavorable circumstances, it may be able to reach a signaling state as in the R92Q mutant. The ligand serves to mitigate this energetic barrier, allowing the ligand-bound receptor to readily adopt an active conformation. Second, ligand mediates network formation. The ligand receptor network, due to it being necessarily coplanar with the membrane, enforces and stabilizes the altered receptor conformation by displacing the ligand binding domain, which in turn causes a conformational change in the transmembrane and cytosolic domains. Additionally, the network may play a role in concentrating the signal or in stabilizing the dimer. We have shown that the R92Q mutant dimerizes with higher affinity than the wild-type; however, it is unknown whether this is a consequence of interactions involving the mutant itself or of its adopted active configuration. If the receptor dimer forms with higher affinity in its active state, it follows that network enforced conformational change would also generate a stronger dimer, amplifying its signaling properties.

Collectively, our results inspire a novel perspective in membrane receptor activation and ligand−receptor network formation. While ligand is known to induce network formation, we have shown that this oligomerization is not enough to explain the signaling event. Rather, by virtue of its formation, the network conspires with the planar membrane to enforce conformational change and receptor activation. Therefore, the relevant signaling event associated with ligand-induced TNFR1 activation involves a conformational change due to collaborative interactions between ligand−receptor, receptor−receptor, and receptor−membrane, which together provide an external force to overcome the energetic barrier between inactive and active states.

■ ASSOCIATED CONTENT

Supporting Information

The backbone *B*-factors of the 1ncf crystal structure (Figure S1), the full cross-correlation maps of the 1ncf and 1tnr normal-mode analyses (Figure S2), our calculation of FRET efficiency (Figure S3), a model of the network structure pitching into the membrane (Figure S4), and alternative FRET analysis (Figure S5). This material is available free of charge via the Internet at http://pubs.acs.org.

■ AUTHOR INFORMATION

Corresponding Author

*Tel (612) 624-7158; Fax (612) 626-6583; e-mail jnsachs@umn.edu.

Notes

The authors declare no competing financial interest.

■ ACKNOWLEDGMENTS

The authors thank Nick Leioatts and Alan Grossfield for invaluable assistance with the LOOS software, the UMN Biophysical Spectroscopy Center, and the Minnesota Supercomputing Institute.

■ ABBREVIATIONS

TNFR1, tumor necrosis factor receptor 1; TRAPS, tumor necrosis factor receptor-associated periodic syndrome; TNF, tumor necrosis factor; LTα, lymphotoxin alpha; SODD, silencer of death domain; TRADD, TNF receptor type 1-associated death domain; NF-κB, nuclear factor κB; FADD, fas associated death domain; TM, transmembrane; PLAD, preligand assembly domain; TRAIL, TNF related apoptosis inducing ligand; DR5, death receptor 5; PDB, protein data bank; CRD, cysteine-rich domain; RMSD, root-mean-square deviation; RMSF, root-mean-square fluctuation; FRET, fluorescence resonance energy transfer; EYFP, enhanced yellow fluorescent protein; ECFP, enhanced cyan fluorescent protein; NMA, normal-mode analysis; ANM, anisotropic network model.

■ REFERENCES

(1) Tansey, M. G., and Szymkowski, D. E. (2009) The TNF superfamily in 2009: new pathways, new indications, and new drugs. *Drug Discovery Today 14*, 1082−1088.

(2) Bhardwaj, A., and Aggarwal, B. B. (2003) Receptor-mediated choreography of life and death. *J. Clin. Immunol. 23*, 317−332.

(3) Croft, M., Duan, W., Choi, H., Eun, S. Y., Madireddi, S., and Mehta, A. (2012) TNF superfamily in inflammatory disease: translating basic insights. *Trends Immunol. 33*, 144−152.

(4) Takei, Y., and Laskey, R. (2008) Tumor necrosis factor alpha regulates responses to nerve growth factor, promoting neural cell survival but suppressing differentiation of neuroblastoma cells. *Mol. Biol. Cell 19*, 855−864.

(5) Ashkenazi, A., and Dixit, V. M. (1998) Death receptors: signaling and modulation. *Science 281*, 1305−1308.

(6) Jiang, Y., Woronicz, J. D., Liu, W., and Goeddel, D. V. (1999) Prevention of constitutive TNF receptor 1 signaling by silencer of death domains. *Science 283*, 543−546.

(7) Hsu, H., Xiong, J., and Goeddel, D. V. (1995) The TNF receptor 1-associated protein TRADD signals cell death and NF-kappa B activation. *Cell 81*, 495−504.

(8) Wajant, H., and Scheurich, P. (2011) TNFR1-induced activation of the classical NF-κB pathway. *FEBS J. 278*, 862−876.

(9) Hsu, H., Shu, H. B., Pan, M. G., and Goeddel, D. V. (1996) TRADD-TRAF2 and TRADD-FADD interactions define two distinct TNF receptor 1 signal transduction pathways. *Cell 84*, 299−308.

(10) Deng, G. M., Zheng, L., Chan, F. K., and Lenardo, M. (2005) Amelioration of inflammatory arthritis by targeting the pre-ligand assembly domain of tumor necrosis factor receptors. *Nat. Med. 11*, 1066−1072.

(11) Kimberley, F. C., Lobito, A. A., Siegel, R. M., and Screaton, G. R. (2007) Falling into TRAPS–receptor misfolding in the TNF receptor 1-associated periodic fever syndrome. *Arthritis Res. Ther. 9*, 217.

(12) Hadziselimovic, F., Emmons, L. R., and Gallati, H. (1995) Soluble tumour necrosis factor receptors p55 and p75 in the urine monitor disease activity and the efficacy of treatment of inflammatory bowel disease. *Gut 37*, 260−263.

(13) Poirier, O., Nicaud, V., Gariépy, J., Courbon, D., Elbaz, A., Morrison, C., Kee, F., Evans, A., Arveiler, D., Ducimetière, P., Amarenco, P., and Cambien, F. (2004) Polymorphism R92Q of the tumour necrosis factor receptor 1 gene is associated with myocardial infarction and carotid intima-media thickness–the ECTIM, AXA, EVA and GENIC Studies. *Eur. J. Hum. Genet. 12*, 213−219.

(14) Amoura, Z., Dodé, C., Hue, S., Caillat-Zucman, S., Bahram, S., Delpech, M., Grateau, G., Wechsler, B., and Piette, J. C. (2005) Association of the R92Q TNFRSF1A mutation and extracranial deep vein thrombosis in patients with Behçet's disease. *Arthritis Rheum. 52*, 608−611.

(15) Caminero, A., Comabella, M., and Montalban, X. (2011) Role of tumour necrosis factor (TNF)-α and TNFRSF1A R92Q mutation in the pathogenesis of TNF receptor-associated periodic syndrome and multiple sclerosis. *Clin. Exp. Immunol. 166*, 338−345.
(16) Lobito, A. A., Kimberley, F. C., Muppidi, J. R., Komarow, H., Jackson, A. J., Hull, K. M., Kastner, D. L., Screaton, G. R., and Siegel, R. M. (2006) Abnormal disulfide-linked oligomerization results in ER retention and altered signaling by TNFR1 mutants in TNFR1-associated periodic fever syndrome (TRAPS). *Blood 108*, 1320−1327.
(17) Chen, Y. F., Jobanputra, P., Barton, P., Jowett, S., Bryan, S., Clark, W., Fry-Smith, A., and Burls, A. (2006) A systematic review of the effectiveness of adalimumab, etanercept and infliximab for the treatment of rheumatoid arthritis in adults and an economic evaluation of their cost-effectiveness. *Health Technol. Assess. 10*, 1−229 , iii−iv, xi−xiii.
(18) Chan, F. K., Chun, H. J., Zheng, L., Siegel, R. M., Bui, K. L., and Lenardo, M. J. (2000) A domain in TNF receptors that mediates ligand-independent receptor assembly and signaling. *Science 288*, 2351−2354.
(19) Goh, C. R., Loh, C. S., and Porter, A. G. (1991) Aspartic acid 50 and tyrosine 108 are essential for receptor binding and cytotoxic activity of tumour necrosis factor beta (lymphotoxin). *Protein Eng. 4*, 785−791.
(20) Banner, D. W., D'Arcy, A., Janes, W., Gentz, R., Schoenfeld, H. J., Broger, C., Loetscher, H., and Lesslauer, W. (1993) Crystal structure of the soluble human 55 kd TNF receptor-human TNF beta complex: implications for TNF receptor activation. *Cell 73*, 431−445.
(21) Valley, C. C., Lewis, A. K., Mudaliar, D. J., Perlmutter, J. D., Braun, A. R., Karim, C. B., Thomas, D. D., Brody, J. R., and Sachs, J. N. (2012) Tumor necrosis factor-related apoptosis-inducing ligand (TRAIL) induces Death Receptor 5 networks that are highly organized. *J. Biol. Chem.*, in press.
(22) Chan, F. K. (2007) Three is better than one: pre-ligand receptor assembly in the regulation of TNF receptor signaling. *Cytokine 37*, 101−107.
(23) Loetscher, H., Gentz, R., Zulauf, M., Lustig, A., Tabuchi, H., Schlaeger, E. J., Brockhaus, M., Gallati, H., Manneberg, M., and Lesslauer, W. (1991) Recombinant 55-kDa tumor necrosis factor (TNF) receptor. Stoichiometry of binding to TNF alpha and TNF beta and inhibition of TNF activity. *J. Biol. Chem. 266*, 18324−18329.
(24) Naismith, J. H., and Sprang, S. R. (1998) Modularity in the TNF-receptor family. *Trends Biochem. Sci. 23*, 74−79.
(25) Naismith, J. H., Devine, T. Q., Brandhuber, B. J., and Sprang, S. R. (1995) Crystallographic evidence for dimerization of unliganded tumor necrosis factor receptor. *J. Biol. Chem. 270*, 13303−13307.
(26) Branschädel, M., Aird, A., Zappe, A., Tietz, C., Krippner-Heidenreich, A., and Scheurich, P. (2010) Dual function of cysteine rich domain (CRD) 1 of TNF receptor type 1: conformational stabilization of CRD2 and control of receptor responsiveness. *Cell. Signalling 22*, 404−414.
(27) Ozsoy, H. Z., Sivasubramanian, N., Wieder, E. D., Pedersen, S., and Mann, D. L. (2008) Oxidative stress promotes ligand-independent and enhanced ligand-dependent tumor necrosis factor receptor signaling. *J. Biol. Chem. 283*, 23419−23428.
(28) Scott, F. L., Stec, B., Pop, C., Dobaczewska, M. K., Lee, J. J., Monosov, E., Robinson, H., Salvesen, G. S., Schwarzenbacher, R., and Riedl, S. J. (2009) The Fas-FADD death domain complex structure unravels signalling by receptor clustering. *Nature 457*, 1019−1022.
(29) Tama, F., and Sanejouand, Y. H. (2001) Conformational change of proteins arising from normal mode calculations. *Protein Eng. 14*, 1−6.
(30) Zheng, W., and Brooks, B. R. (2005) Normal-modes-based prediction of protein conformational changes guided by distance constraints. *Biophys. J. 88*, 3109−3117.
(31) Wang, M., Borchardt, R. T., Schowen, R. L., and Kuczera, K. (2005) Domain motions and the open-to-closed conformational transition of an enzyme: a normal mode analysis of S-adenosyl-L-homocysteine hydrolase. *Biochemistry 44*, 7228−7239.
(32) Humphrey, W., Dalke, A., and Schulten, K. (1996) VMD: visual molecular dynamics. *J. Mol. Graphics 14* (33−38), 27−38.
(33) Romo, T. D., and Grossfield, A. (2009) LOOS: an extensible platform for the structural analysis of simulations. *Conf. Proc. IEEE Eng. Med. Biol. Soc.*, 2332−2335.
(34) Zacharias, D. A., Violin, J. D., Newton, A. C., and Tsien, R. Y. (2002) Partitioning of lipid-modified monomeric GFPs into membrane microdomains of live cells. *Science 296*, 913−916.
(35) Atilgan, A. R., Durell, S. R., Jernigan, R. L., Demirel, M. C., Keskin, O., and Bahar, I. (2001) Anisotropy of fluctuation dynamics of proteins with an elastic network model. *Biophys. J. 80*, 505−515.
(36) Petrone, P., and Pande, V. S. (2006) Can conformational change be described by only a few normal modes? *Biophys. J. 90*, 1583−1593.
(37) Marques, O., and Sanejouand, Y. H. (1995) Hinge-bending motion in citrate synthase arising from normal mode calculations. *Proteins 23*, 557−560.
(38) Ma, J., and Karplus, M. (1997) Ligand-induced conformational changes in ras p21: a normal mode and energy minimization analysis. *J. Mol. Biol. 274*, 114−131.
(39) Van Wynsberghe, A. W., and Cui, Q. (2006) Interpreting correlated motions using normal mode analysis. *Structure 14*, 1647−1653.
(40) Rebelo, S. L., Bainbridge, S. E., Amel-Kashipaz, M. R., Radford, P. M., Powell, R. J., Todd, I., and Tighe, P. J. (2006) Modeling of tumor necrosis factor receptor superfamily 1A mutants associated with tumor necrosis factor receptor-associated periodic syndrome indicates misfolding consistent with abnormal function. *Arthritis Rheum. 54*, 2674−2687.
(41) Li, M., Reddy, L. G., Bennett, R., Silva, N. D., Jones, L. R., and Thomas, D. D. (1999) A fluorescence energy transfer method for analyzing protein oligomeric structure: application to phospholamban. *Biophys. J. 76*, 2587−2599.
(42) Kelly, E. M., Hou, Z., Bossuyt, J., Bers, D. M., and Robia, S. L. (2008) Phospholamban oligomerization, quaternary structure, and sarco(endo)plasmic reticulum calcium ATPase binding measured by fluorescence resonance energy transfer in living cells. *J. Biol. Chem. 283*, 12202−12211.
(43) Autry, J. M., Rubin, J. E., Pietrini, S. D., Winters, D. L., Robia, S. L., and Thomas, D. D. (2011) Oligomeric interactions of sarcolipin and the Ca-ATPase. *J. Biol. Chem. 286*, 31697−31706.
(44) Kim, M., Carman, C. V., and Springer, T. A. (2003) Bidirectional transmembrane signaling by cytoplasmic domain separation in integrins. *Science 301*, 1720−1725.
(45) Ishikawa-Ankerhold, H. C., Ankerhold, R., and Drummen, G. P. (2012) Advanced fluorescence microscopy techniques–FRAP, FLIP, FLAP, FRET and FLIM. *Molecules 17*, 4047−4132.
(46) Sukits, S. F., Lin, L. L., Hsu, S., Malakian, K., Powers, R., and Xu, G. Y. (2001) Solution structure of the tumor necrosis factor receptor-1 death domain. *J. Mol. Biol. 310*, 895−906.
(47) Telliez, J. B., Xu, G. Y., Woronicz, J. D., Hsu, S., Wu, J. L., Lin, L., Sukits, S. F., Powers, R., and Lin, L. L. (2000) Mutational analysis and NMR studies of the death domain of the tumor necrosis factor receptor-1. *J. Mol. Biol. 300*, 1323−1333.
(48) Zhu, J., Carman, C. V., Kim, M., Shimaoka, M., Springer, T. A., and Luo, B. H. (2007) Requirement of alpha and beta subunit transmembrane helix separation for integrin outside-in signaling. *Blood 110*, 2475−2483.
(49) Vilar, M., Charalampopoulos, I., Kenchappa, R. S., Simi, A., Karaca, E., Reversi, A., Choi, S., Bothwell, M., Mingarro, I., Friedman, W. J., Schiavo, G., Bastiaens, P. I., Verveer, P. J., Carter, B. D., and Ibáñez, C. F. (2009) Activation of the p75 neurotrophin receptor through conformational rearrangement of disulphide-linked receptor dimers. *Neuron 62*, 72−83.